Inorg. Chem. **2007**, *46*, 5544–5554

Porphyrin Framework Solids. Synthesis and Structure of Hybrid Coordination Polymers of Tetra(carboxyphenyl)porphyrins and Lanthanide-Bridging Ions

Sankar Muniappan, Sophia Lipstman, Sumod George, and Israel Goldberg*

School of Chemistry, Sackler Faculty of Exact Sciences, Tel-Aviv University, Ramat-Aviv, Tel-Aviv 69978, Israel

Received January 22, 2007

New types of porphyrin-based framework solids were constructed by reacting *meso*-tetra(3-carboxyphenyl)porphyrin and *meso*-tetra(4-carboxyphenyl)metalloporphyrins with common salts of lanthanide metal ions. The large size, high coordination numbers and strong affinity for oxo ligands of the latter, combined with favorable hydrothermal reaction conditions, allowed the formation of open three-dimensional single-framework architectures by coordination polymerization, in which the tetradentate porphyrin units are intercoordinated by multinuclear assemblies of the bridging metal ions. The latter serve as construction pillars of the supramolecular arrays, affording stable structures. Several modes of coordination polymerization were revealed by single-crystal X-ray diffraction. They differ by the spatial functionality of the porphyrin building blocks, the coordination patterns of the lanthanide–carboxylate assemblies, and the topology of the resulting frameworks. The seven new reported structures exhibit periodically spaced 0.4–0.6 nm wide channel voids that perforate the respective crystalline polymeric architectures and are accessible to solvent components. Materials based on the *m*-carboxyphenyl derivative reveal smaller channels than those based on the *p*-carboxyphenyl analogues. An additional complex of the former with a smaller third-row transition metal (Co) is characterized by coordination connectivity in two dimensions only. Thermal and powder-diffraction analyses confirm the stability of the lanthanide–T*m*CPP (T*m*CPP = tetra(*m*-carboxyphenyl)porphyrin) frameworks.

Introduction

Supramolecular chemistry affords a means to predictably construct "bottom up" ordered molecular materials using well-defined algorithms of molecular recognition.[1] Its application to porphyrins, related tetrapyrrolic macrocycles, and other organic ligands has seen tremendous activity in recent years, particularly for the formulation of functional materials.[2−4] We introduced into this field the tetra(carboxyphenyl)porphyrin platform as an extremely versatile building block for the supramolecular synthesis of framework solids.[5,6] It has the potential to self-assemble into two-dimensional (2D) and three-dimensional (3D) architectures not only by multiple complementary (COOH···COOH) hydrogen-bond-

* To whom correspondence should be addressed. E-mail: goldberg@post.tau.ac.il.

(1) *Comprehensive Supramolecular Chemistry*; Atwood, J. L., Davies, J. E. D., MacNicol, D. D., Vögtle, F., Lehn, J.-M., Eds.; Elsevier: Oxford, U.K., and New York, 1996; Vols. 1−11.

(2) For recent reviews on noncovalent assembly of porphyrin arrays and their potential applications see: (a) Chambron, J.-C.; Heitz, V.; Sauvage, J.-P. *The Porphyrin Handbook*; Kadish, K. M., Smith, K. M., Guilard, R., Eds.; Academic Press: Orlando FL, 2000; Vol. 6, Chapter 40, pp 1−42. (b) Chou, J.-H.; Nalwa, H. S.; Kosal, M. E.; Rakow, N. A.; Suslick, K. S. *The Porphyrin Handbook*; Kadish, K. M., Smith, K. M., Guilard, R. Eds.; Academic Press: Orlando FL, 2000; Vol. 6, Chapters 41, 43−132.

(3) Sanders, J. K. M; Bampos, N.; Clyde-Watson, Z; Darling, S. L.; Hawley, J. C.; Kim, H.-J.; Mak, C. C.; Webb, S, J. *The Porphyrin Handbook*; Kadish, K. M., Smith, K. M., Guilard, R., Eds.; Academic Press: London, 2000; Vol. 3, pp 1−48.

(4) (a) Roswell, J. L. C.; Yaghi, O. M. *Angew. Chem., Int. Ed.* **2005**, *44*, 4670−4679. (b) Yaghi, O. M.; O'Keefe, M.; Ockwig, N. W.; Chae, H. K.; Eddaoudi, M.; Kim, J. *Nature* **2003**, *423*, 705−714. (c) Gibb, B. C. A*ngew. Chem., Int. Ed.* **2003**, *42* 1686−1687. (d) Eddaoudi, M.; Kim, J.; Rosi, N.; Vodak, D.; Wachter, J.; O'Keeffe, M.; Yaghi, O. M. *Science* **2002**, *295*, 469−472.

(5) (a) George, S.; Goldberg, I. *Cryst. Growth Des.* **2006**, *6*, 755−762. (b) George, S.; Lipstman, S.; Muniappan, S.; Goldberg, I. *CrystEngComm* **2006**, *8*, 417−424. (c) Diskin-Posner, Y.; Goldberg, I. *Chem. Commun.* **1999**, 1961−1962. (d) Dastidar, P.; Stein, Z.; Goldberg, I. *Supramol. Chem.* **1996**, *7*, 257−270.

(6) (a) Shmilovits, M.; Vinodu, M.; Goldberg, I. *Cryst. Growth Des.* **2004**, *4*, 633−638. (b) Shmilovits, M.; Diskin-Posner, Y.; Vinodu, M.; Goldberg, I. *Cryst. Growth Des.* **2003**, *3*, 855−863. (c) Diskin-Posner, Y.; Dahal, S.; Goldberg, I. *Chem. Commun.* **2000**, 585−586. (d) Diskin-Posner, Y.; Dahal, S.; Goldberg, I. *Angew. Chem., Int. Ed.* **2000**, *39*, 1288−1292.

10.1021/ic0701099 CCC: $37.00
Published on Web 06/13/2007

Scheme 1

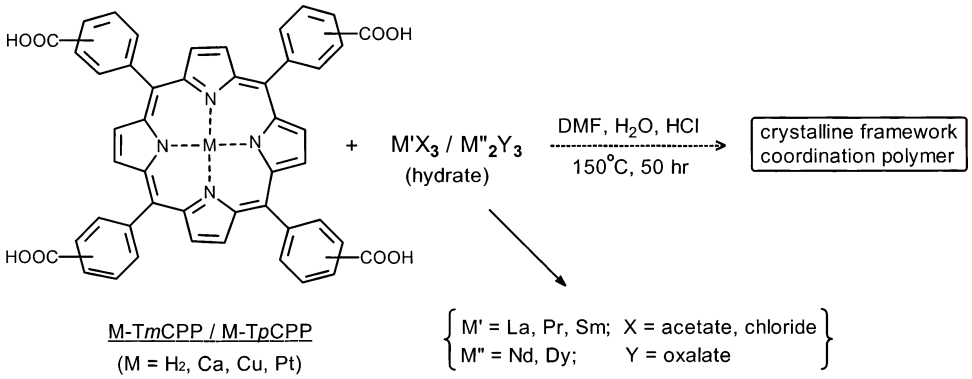

ing patterns but also by intermolecular coordination motifs (COOH/COO^{-}···metal/ligand···^{-}OOC/HOOC) through external auxiliaries.[7] In earlier studies we explored the utility of the tetra(*p*-carboxyphenyl)porphyrin (T*p*CPP) and metalloporphyrin (M−T*p*CPP) derivatives in the supramolecular synthesis of network architectures, either by direct interaction or through bridging organic ligands, metal ions, or clusters of metal ions (including alkali and third-row transition metals). The various reported examples attest to the high propensity of the T*p*CPP scaffold to assemble into tuneable open, zeolite-like, framework architectures that are suitable to incorporate guest components.[7] Importantly, in the above context, the T*p*CPP networking by intercoordination via exocyclic metal bridges does not require the introduction of foreign counterions into the lattice, as the charge is readily balanced by either full or partial deprotonation of the porphyrin tetraacid. This is advantageous to the possible formulation of T*p*CPP-based robust functional microporous solids (without the interference of the anionic species that come with the metal cations), sustained by multiple interactions between the carboxylate groups of neighboring porphyrin species and bridging metal ion clusters.[8] Coordination polymerization in three dimensions is the preferred venue for the formulation of sturdy materials. Within the latter context, we found most recently that lanthanide ions provide a very attractive interface to promote the formation of stable 3D-framework coordination polymers with free-base T*p*CPP.[9] This is due to their large size, spatial divergence of the valent orbitals, and high CNs—up to nine for their most abundant oxidation state of +3 ("CN" denotes coordination number). Then, the "hard" lanthanide ions reveal a high affinity for oxo ligands, and even as simple acetates or oxalates, they tend to form polynuclear aggregates bridged by several anions.[10] Our synthetic efforts have led to the successful construction of robust single-framework lanthanide-T*p*CPP coordination polymers in the solid state. The coordination patterns in these solids fall into three different categories according to the nuclearity (polynuclear, tetranuclear, and binuclear) of the interporphyrin metal−carboxylate bridging assemblies.[9] Along the same line of reasoning, we focus our attention in the present account on the tessellation of the tetra(*m*-carboxyphenyl)porphyrin (T*m*CPP) scaffold with lanthanide ions into closely related polymeric architectures but characterized by a different directionality of the coordination bonds due to the meta rather than para disposition of the carboxylate functions on the phenyl rings. This allows an examination of how the assembly modes and the "porosity" of the resulting structures is affected by the different functionalization of the porphyrin platform and provides a significant expansion of the scope of materials that can be formed. The possible participation of additional anionic species that originate from the commercially available lanthanide salts and/or the experimental conditions in the coordination polymerization will be also discussed. The available crystalline solids that could be reliably analyzed in the present study include hybrid polymers of T*m*CPP with La^{III} (1:1), Pr^{III} (2:1), Pr^{III} (1:1), and Sm^{III} (1:1) ions (compounds **1**−**4**, respectively). Another example involves a 2:1 polymer of T*m*CPP with Dy^{III} (**5**), in which additional oxalate anions are incorporated as spacers into the supramolecular coordination scheme. For comparison, two new materials involving the metalated T*p*CPP platform of Cu−T*p*CPP with Dy^{III} and oxalate bridging ions (1:1:1; **6**), and of Pt−T*p*CPP and Nd^{III} ions (3:4; **7**), are included in this report. Also reported is a polymeric compound of Co−T*m*CPP with Co^{III} ions, as interporphyrin connectors (1:1; **8**), which reveals a coordination pattern only in two dimensions. Details of the synthetic procedures are discussed.

Results and Discussion

The metal−T*m*CPP/T*p*CPP coordination polymers were prepared by the hydrothermal technique, which involves reacting the porphyrin moiety (dissolved in DMF (DMF = dimethylformamide)—occasionally dilute aqueous potassium hydroxide solution is added to enhance deprotonation of the carboxylic groups) with a given lanthanide salt (dissolved in dilute HCl to increase its reactivity) in a sealed reactor at 150 °C for about 50 h. In most cases, these experimental conditions provide an optimal environment for the construc-

(7) (a) Goldberg, I. *Chem. Commun.* **2005**, 1243−1254. (b) Goldberg, I. *Chem.—Eur. J.* **2000**, *6*, 3863−3870.

(8) (a) Suslick, K. S.; Byrappa, P.; Chou, J.-H.; Kosal, M. E.; Nakagaki, S.; Smitherny, W. D.; Wilson, S. R. *Acc. Chem. Res.* **2005**, *38*, 283−291. (b) Smitherny, W. D.; Wilson, S. R.; Suslick, K. S. *Inorg. Chem.* **2003**, *42*, 7719−7721. (c) Kosal, M. E.; Chou, J.-H.; Wilson, S. R.; Suslick, K. S. *Nat. Mat.* **2002**, *1*, 118−121.

(9) (a) George, S.; Lipstman, S.; Goldberg, I. *Cryst. Growth Des.* **2006**, *6*, 2651−2654. (b) Lipstman, S.; Muniappan, S.; George, S.; Goldberg, I. *Dalton Trans.* **2007**, in press.

(10) This is evidenced by numerous structures of the lanthanide salts with acetate, oxalate, and other small carboxylate anions, which are archived in the Cambridge Structural Database. Allen, F. *Acta Crystallogr.* **2002**, *B32*, 380−388.

Table 1. Crystal and Experimental Data for Structures **1**−**4**[a]

	1[a]	**2**[a]	**3**[a]	**4**[a]
formula	$C_{48}H_{28}Ca_{0.19}LaN_4O_{10}$	$C_{25}H_{16}N_2O_7Pr$	$C_{48}H_{31}N_4O_{10}Pr$	$C_{48}H_{28}Ca_{0.18}N_4O_{10}Sm$
fw	967.47	597.31	964.68	979.11
cryst syst	monoclinic	triclinic	triclinic	triclinic
space group	$P2_1/c$	$P\bar{1}$	$P\bar{1}$	$P\bar{1}$
a [Å]	13.8138(2)	7.4595(1)	9.6357(2)	9.6187(3)
b [Å]	33.7925(7)	11.4740(3)	13.9203(3)	13.8934(6)
c [Å]	9.8548(3)	16.4767(4)	17.2875(5)	17.2345(7)
α [deg]	90.0	98.9511(11)	98.1574(9)	98.058(2)
β [deg]	92.863(1)	90.9863(14)	89.7511(9)	90.457(2)
γ [deg]	90.0	91.3109(14)	89.1062(16)	90.599(3)
V [Å^3]	4594.5(2)	1392.40(5)	2295.0(1)	2280.2(2)
Z	4	2	2	2
ρ_{calcd} [Mg m^{-3}]	1.399	1.425	1.396	1.426
μ [mm^{-1}]	1.012	1.790	1.122	1.371
F(000)	1940	590	972	980
crystal size [mm^3]	0.50 × 0.15 × 0.05	0.45 × 0.10 × 0.10	0.20 × 0.10 × 0.05	0.30 × 0.10 × 0.10
θ_{max} [deg]	27.48	28.18	25.66	28.29
reflns collected	35 923	13 003	19 543	21 301
reflns unique	10 518	6475	8568	10 704
R(int)	0.097	0.026	0.059	0.047
completeness [%]	100	95	99	95
reflns with $I>2\sigma(I)$	5694	5858	6797	8558
refined parameters	575	317	570	566
R1 [$I>2\sigma(I)$][b]	0.049 (0.081)	0.035 (0.051)	0.042 (0.082)	0.050 (0.093)
wR2 [$I>2\sigma(I)$][b]	0.108 (0.267)	0.098 (0.152)	0.094 (0.225)	0.112 (0.251)
R1 [all data][b]	0.106 (0.150)	0.039 (0.057)	0.057 (0.101)	0.067 (0.113)
wR2 [all data][b]	0.120 (0.305)	0.101 (0.156)	0.100 (0.241)	0.118 (0.265)
± $\Delta\rho_{max}$ [e Å^{-3}]	+2.95, −1.13	+3.16, −1.27	+1.48, −1.22	+1.60, −1.33
solvent accessible void space [Å^3]	894.3 (19.5%)	340.1 (24.4%)	414.1 (18.0%)	418.3 (18.3%)

[a] Excluding the noninteracting solvent diffused within the interporphyrin channels (see the Experimental Section). [b] Data in parentheses refer to refinements based on the uncorrected diffraction data.

tion of robust framework solids. They ensure complete (or almost complete) replacement of the anions present in the original metal reagent by the formation of multiple linkages to the carboxylate functions of the porphyrin T*m*CPP and T*p*CPP species. Moreover, hydrothermal conditions often favor the crystallization of high nuclearity products (i.e., formation of the desired metal ion clusters) in good yields.[4d,11] Finally, the reactions were carried out in a DMF−water solvent environment, as hydrolysis of the DMF (to the appropriate amine with the release of formate HCO_2^- anion) was found to promote the synthesis of metal−organic frameworks.[12] In a small number of cases, additional species (from the solvent or metal impurities often present in commercially available lanthanide salts) were found inserted into the porphyrin core, without affecting the supramolecular organization. Moreover, the possibility of the incorporation of other carboxylate anions (e.g., oxalate) that are present in the reaction mixture as part of the used lanthanide reagent (e.g., in the commercially available dysprosium oxalate hydrate) is also possible.

The afforded new crystalline products **1**−**7** were characterized by single-crystal X-ray diffraction. The crystallographic and experimental data are given in Tables 1 and 2. All structures represent the coordination polymerization of hybrid T*m*CPP/T*p*CPP−metal arrays, wherein the lanthanide ions bridge several deprotonated porphyrin moieties. The coordination distances, which are listed in Table 3, are indicative of strong interactions between the component species. The various trivalent lanthanide ions exhibit, as expected, high CNs (≥7), supplementing their coordination sphere by molecules of the water and occasionally by other small carboxylate anions.

The coordination scheme characteristic to compound **1** is depicted schematically in Figure 1. It represents a continuous interaction synthon that propagates throughout the crystal lattice, wherein every lanthanide ion binds to the lateral carboxylate functions of six different neighboring T*m*CPP units, four of which bridge two consecutive metals along the chain. The coordination sphere of the latter includes six carboxylic/carboxylate O atoms and two additional molecules of water at each metal node. Three of the carboxylic acid groups at every T*m*CPP site are deprotonated to balance the 3+ charge of the lanthanide cation. Two cis-related functions point upward above the porphyrin core, the two other groups being directed downward below the porphyrin core. They associate directly with six different metal centers, with two carboxylates binding simultaneously to two metal ions, while each of the other COO^- and COOH functions coordinate to a single metal site. The continuous pattern of the coordination bonds in four different directions at the four corners of the T*m*CPP unit results in the formation of a supramolecular porphyrin network of 3D topology (Figure 2). It is composed of wavy layers of intercoordinated porphyrins (instead of flat networks observed in the corresponding T*p*CPP-based structures),[9a] which adopt a herringbone organization, expanding parallel to the *ab* plane of the crystal. These layers

(11) Low, D. M.; Jones, L. F.; Bell, A.; Brechin, E. K.; Mallah, T.; Riviere, E.; Teat, S. J.; McInnes, E. J. L. *Angew. Chem., Int. Ed.* **2003**, *42*, 3791−3784.
(12) Burrows, A. D.; Cassar, K.; Friend, R. M. W.; Mahon, M. F.; Rigby, S. P.; Warren, J. E. *CrystEngComm* **2005**, *7*, 548−550.

Table 2. Crystal and Experimental Data for Structures **5**−**8**

	5[a]	**6**[a]	**7**[a]	**8**
formula	$C_{52}H_{30}Dy_2N_4O_{18}$	$C_{49}H_{25}CuDyN_4O_{10}$	$C_{75}H_{46}N_7Nd_2O_{14}Pt_{1.5}$	$C_{52}H_{41.4}Co_2N_6O_{8.7}$
fw	1323.80	991.03	1850.30	1007.37
crystal system	monoclinic	triclinic	monoclinic	triclinic
space group	$P2_1/c$	$P\bar{1}$	$C2/c$	$P\bar{1}$
a [Å]	18.6144(4)	9.5168(2)	21.6348(6)	9.0754(4)
b [Å]	27.9022(9)	15.0535(3)	24.1366(7)	14.5477(5)
c [Å]	11.7735(8)	18.0806(4)	31.3773(6)	17.2021(8)
α [deg]	90.0	92.623(1)	90.0	73.888(2)
β [deg]	100.085(1)	103.711(1)	104.292(2)	85.612(2)
γ [deg]	90.0	95.606(1)	90.0	81.146(3)
V [Å^3]	6020.5(5)	2498.0(1)	15877.8(7)	2154.6(2)
Z	4	2	8	2
ρ_{calcd} [Mg m^{-3}]	1.460	1.404	1.548	1.553
μ [mm^{-1}]	2.530	1.967	3.985	0.840
F(000)	2584	1044	7152	1038
cryst size [mm^3]	0.20 × 0.20 × 0.20	0.40 × 0.05 × 0.05	0.45 × 0.10 × 0.10	0.20 × 0.20 × 0.15
θ_{max} [deg]	25.00	25.68	28.21	27.50
reflns collected	40 763	21 764	52 701	18 626
reflns unique	10 536	9364	19 076	9213
R(int)	0.109	0.073	0.072	0.088
completeness [%]	100	98	97	93
reflns with $I>2\sigma(I)$	5297	7300	10 440	6516
refined params	687	586	815	643
R1 [$I>2\sigma(I)$][b]	0.069 (0.125)	0.052 (0.085)	0.064 (0.083)	0.066
wR2 [$I>2\sigma(I)$][b]	0.172 (0.351)	0.128 (0.232)	0.164 (0.228)	0.126
R1 [all data][b]	0.124 (0.246)	0.071 (0.109)	0.116 (0.154)	0.105
wR2 [all data][b]	0.191 (0.413)	0.136 (0.250)	0.180 (0.268)	0.143
± $\Delta\rho_{max}$ [e Å^{-3}]	+6.10, −1.69	+1.57, −2.27	+4.69, −1.76	+0.55, −0.54
solvent accessible void space [Å^3]	1673.8 (27.8%)	756.6 (30.3%)	4578.8 (28.8%)	−

[a] Excluding the noninteracting solvent diffused within the interporphyrin channels (see the Experimental Section). [b] Data in parentheses refer to refinements based on the uncorrected diffraction data.

Table 3. Topology of the Bridging Metal Coordination in Compounds **1**−**8**

compound (type of metal)	M···O coordination distance range (Å)	nuclearity of the coordination synthon	metal:TCPP stoichiometry[a]	CN of the metal ions	M···M distances (Å)
1 (La)	2.407(3)−2.661(3)	polymeric	1:1	8	4.928[b]
2 (Pr)	2.413(2)−2.692(3)	polymeric	2:1	8	4.029[c], 4.199[b]
3 (Pr)	2.362(2)−2.597(3)	dimeric	1:1	8	5.276[b]
4 (Sm)	2.320(3)−2.559(3)	dimeric	1:1	8	5.251[b]
5 (Dy)	2.320(6)−2.567(7)	polymeric	2:1	9	6.140[d]
6 (Dy)	2.293(4)−2.606(4)	polymeric	1:1	8	4.182[e], 6.188[d]
7 (Nd)	2.347(6)−2.664(11)	tetrameric	4:3	7 and 8	4.089[b], 4.168[e]
8 (Co)	2.017(3)−2.294(3)	monomeric	1:1	5	

[a] The TCPP units are either triply or quadruply deprotonated to balance the charge of the interacting M^{III} ions. [b] Metal ions are bridged by two carboxylate functions. [c] Metal ions are bridged by two carboxylate and two formate anions. [d] Metal ions are coordinated through an oxalate spacer. [e] Metal ions are bridged by four carboxylate groups.

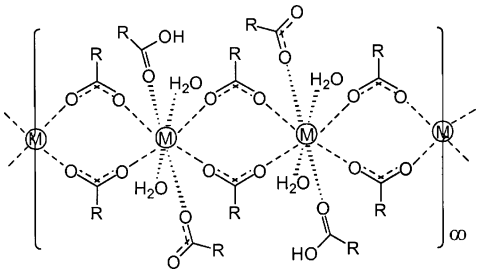

Figure 1. Schematic illustration of the coordination-polymerization mode in compound **1**. "M" symbolizes the La^{III} ions, and "R" represents the porphyrin framework associated with the shown carboxylic/carboxylate group.

are tessellated to one another along the *c* direction by periodically spaced polymeric metal−carboxylate synthons that act as construction pillars. A view down these pillars is depicted in Figure 3, also revealing the solvent-accessible void space present in a thus-formed lattice. Numerous hydrogen bonds between the water ligands and the COOH/COO^- groups of adjacent species assist in the stabilization of the observed architecture. The coordination sphere around every La ion consists of six COOH/COO− ligands at La−O(porphyrin) distances below 2.57 Å and the two more weakly bound water sites at La−O(water) = 2.65−2.66 Å (CN = 8). Details on the coordination bonds are summarized in Table 3.

The polymeric lattice of crystalline **1** is characterized by narrow (approximately 0.4−0.5 nm wide) solvent-accessible channel voids (centered at $x = {}^1/_2$, $y = {}^1/_4$ and $x = {}^1/_2$, $y = {}^3/_4$) that propagate through it parallel to the *c* axis. They consist of only about 19% of the crystal volume (Table 1), attesting to a considerably less "porous" architecture than in comparable framework polymers based on the T*p*CPP platform.[9] This is consistent with the wavy-herringbone vs the flat topologies of the laterally networked polymeric

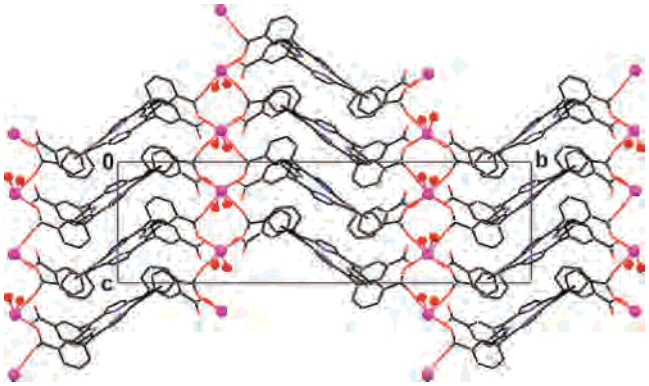

Figure 2. Supramolecular La−T*m*CPP coordination polymer of **1**, viewed down the *a* axis of the crystal. The metal ions and the water ligands bound to them are denoted by small spheres. Note the continuous binding pattern, the marked twist of the porphyrin core, and the tight herringbone arrangement of the porphyrin units. The hydrogen atoms and the impurity metals residing in the porphyrin core have been omitted for clarity.

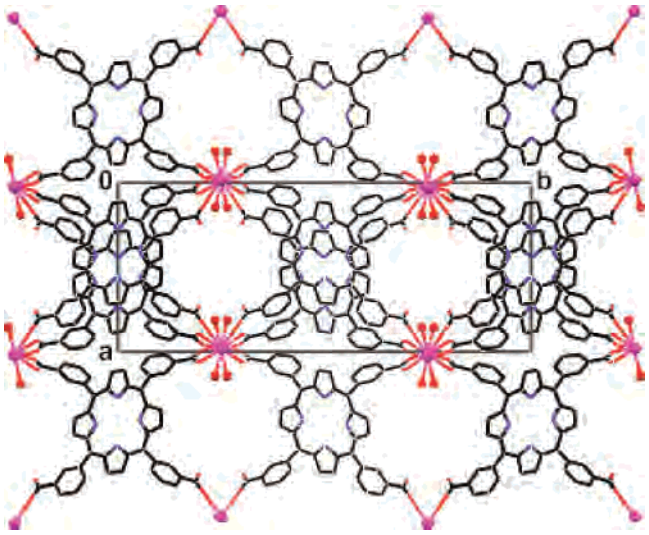

Figure 3. Crystal structure of **1**, viewed down the *c* axis and down the metal−carboxylate coordination chains at $0,^{1}/_{4},z$ and $0,^{3}/_{4},z$ (stick diagram). Only the metal ions and the water ligands bound to them are denoted by small spheres. Note the solvent-accessible voids, which propagate through the crystal parallel to *c*.

assemblies in the T*m*CPP and T*p*CPP materials, the latter being characterized by wider interporphyrin voids (see also below).

A slightly different variant of the continuous metal−carboxylate coordination synthon characterizes framework polymer **2**, which has a 1:2 porphyrin−metal stoichiometry (Figure 4).

As in the previous example, it involves chains of the metal ions (Pr^{III}), in which adjacent metals are doubly bridged by the porphyrin−carboxylate functions (Table 3). However, in the present case, every other pair of the metal sites is further doubly bridged by formate anions that are present in the reaction mixture (as a result of DMF hydrolysis). The latter replace the R−COOH, R−COO^{-}, and one of the water ligands, which are part of the coordination scheme in the earlier example (see Figure 1). Another modification of the coordination pattern in **2** is that all four carboxyphenyl substituents of a given T*m*CPP unit now bridge two adjacent Pr ions. As a result, the unique Pr···Pr distances along the

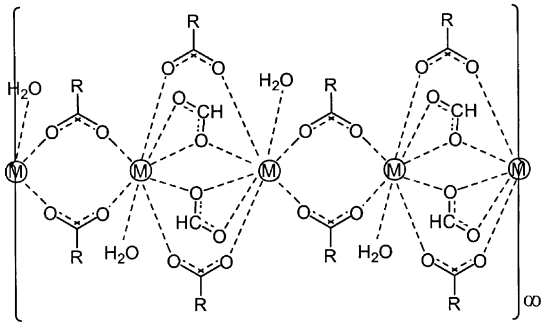

Figure 4. Schematic illustration of the polymeric coordination pattern in **2**. "M" symbolizes the Pr^{III} ions, and "R" represents the porphyrin framework associated with the COO^{-} group it is attached to. Note the two formate ions that bridge every other pair of the metal sites. The coordination bonds are denoted by dashed lines. A water molecule is also ligated to every metal ion along the chain, the latter exhibiting CN = 8.

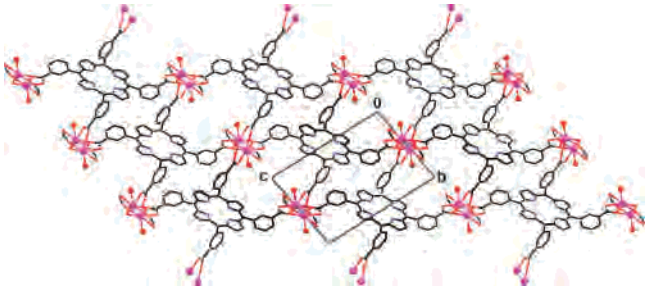

Figure 5. Crystal structure of **2** projected down the *a* axis of the crystal and down the metal−carboxylate coordination chains at $x,^{1}/_{2},0$. The metal ions and the water ligands bound to them are denoted by small spheres. Note that each porphyrin unit connects to four different chains and that porphyrins at different *x* levels (which are overlapped in this projection) connect to the same chains.

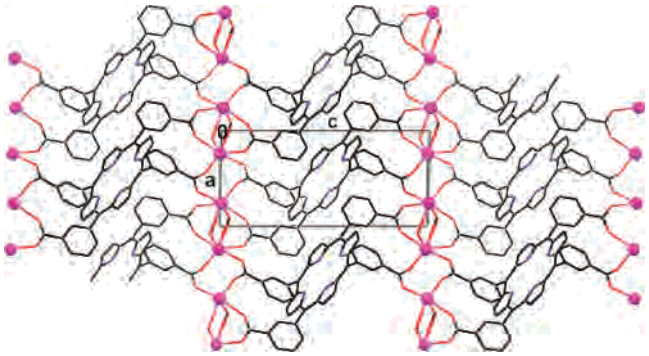

Figure 6. Crystal structure **2** viewed down the *b* axis of the crystal. The metal ions are denoted by small spheres (water ligands and H atoms are omitted). Note the continuous coordination pattern and the intermetal bridging by the formate ions (only a half porphyrin is shown in the upper right and lower left corners). To avoid confusion, note also that the metal−carboxylate chains displaced along ±*b* axis completely overlap in this projection, keeping in mind that every T*m*CPP unit connects to four such chains.

polymeric chain are now 4.029 and 4.199 Å, considerably shorter than the 4.928 Å La···La distances along the polymeric array in **1**.

Two views of the crystal structure are shown in Figures 5 and 6. The coordination patterns (pillars) shown in Figure 4 are aligned in the crystal parallel to the *a* axis at $x,^{1}/_{2},0$. Every porphyrin unit connects to four different chains displaced with respect to one another along *b* and *c* (Figure 5). Then, parallel porphyrin scaffolds displaced along ±*a* coordinate to the same pillars (Figure 6), thus yielding a single-

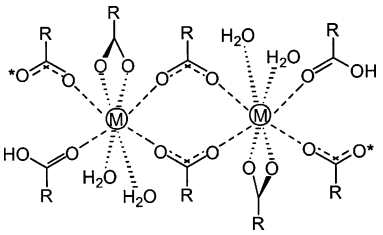

Figure 7. Schematic illustration of the dinuclear coordination pattern in the isomorphous structures **3** and **4**. "M" symbolizes the Pr^{III}/Sm^{III} ions, and "R" represents the porphyrin framework associated with the COOH/COO^- group it is attached to. Every metal ion coordinates to eight ligating sites (CN = 8). Dashed lines denote the coordination bonds. The asterisked O sites are hydrogen bonded to one of the water ligands in adjacent dinuclear clusters.

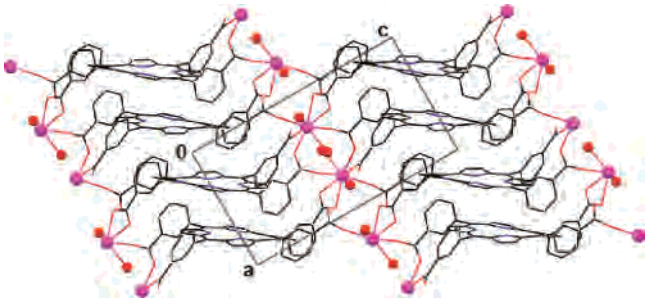

Figure 8. Supramolecular M−T*m*CPP coordination polymer of **3**/**4**, viewed down the *b* axis of the crystal. The metal ions and the water ligands bound to them are denoted by small spheres. The H atoms and the impurity metals (in **4**) residing in the porphyrin core have been omitted for clarity. Note that the regular alignment of the porphyrin units and the carboxylate-bridged dinuclear clusters is similar to that observed in **1**.

framework architecture fully sustained in three dimensions by metal−ligand coordination. As in **1**, narrow channels accessible to solvent species perforate the entire structure. They are centered at 0,0,0, propagating parallel to *a*.

As opposed to the chain-type metal−carboxylate associations in **1** and **2**, the isomorphous triclinic solids **3** and **4** exhibit dinuclear binding schemes (Figure 7). They are characterized by CN = 8 about the metal centers and 1:1 metal−T*m*CPP stoichiometries. The two metal ions (Pr^{III} in **3** and Sm^{III} in **4**) in the assembled cluster are bridged by two coordinating carboxylate moieties, and the distances between them are 5.276 Å in **3** and 5.251 Å in **4**. Each one of them is coordinated further to three COOH/COO^- sites and two water ligands at M−O ≤ 2.60 Å.

Although in this case the metal−carboxylate coordination scheme is limited to a finite number of interacting species (rather than forming a continuous chain), the resulting polymeric architectures still preserve the 3D framework connectivity features. This is because every T*m*CPP unit coordinates simultaneously to several metal sites. One $PhCOO^-$ arm bridges two metals, while the other three PhCOOH/$PhCOO^-$ functions connect either singly or doubly to yet three different metal ions. In addition, hydrogen bonding occurs between the water molecules of one dinuclear cluster to the carboxylate functions of adjacent clusters. The intermolecular organization in **3** and **4** is illustrated in Figures 8 and 9. Interestingly, the regular alignment of the porphyrin units and the carboxylate-bridged lanthanide metal clusters is generally similar to that observed in **1**, with the exception that in the triclinic system the different cascaded zones of

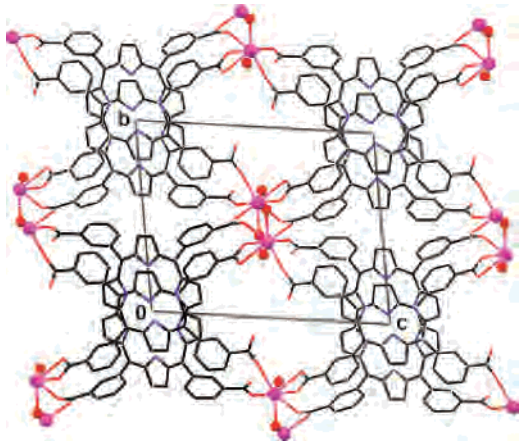

Figure 9. Crystal structure of **3**/**4** viewed down the *a* axis. The metal ions and the water ligands bound to them are denoted by small spheres. Note the solvent-accessible voids, which propagate through the crystal parallel to *a*, at $x,0,{}^1/_2$.

the former are oriented parallel to one another (and not in a herringbone fashion). The resemblance is striking when both structure types are viewed down the axes of the intralattice channel voids (compare Figure 3 and Figure 9). As in **1**, ∼0.45 nm wide solvent-accessible channels that propagate parallel to the *a*-axis of the latter crystals perforate the overall polymeric lattices of **3** and **4**.

Evidently, the framework coordination polymerization (rather than the formation of discrete complexes) represents a thermodynamically preferred mode of intermolecular organization due to the high gain in enthalpy of the numerous bonds that form. To facilitate this in all structures, the functional carboxyphenyl substituents arrange in a "chair" conformation (see below), with the two pairs of cis-related groups oriented in opposite directions with respect to the mean porphyrin plane. (Moreover, the porphyrin core in the different structures is deformed from planarity to a varying degree to optimize the coordinative bonds.) In principle, two other configurational isomers of T*m*CPP are possible: (1) a structure with all *m*-carboxyphenyl groups turned in the same direction (either up or down with respect to the porphyrin core), which may not be favored by entropy; or (2) porphyrin species with trans-related *m*-carboxyphenyl functions pointing up and the other two down, representing a tetrahedral functionality, which may lead to interwoven arrays of diamondoid topology. Their formation is probably characterized by relatively slow kinetics, in the presence of competing options associated with similar enthalpy features (due to a little constrained rotation of the *m*-carboxyphenyl groups around the bonds connecting them to the porphyrin core). The "chairlike" configuration was encountered in all the reaction products **1**−**5**. It leads to zigzag- or herringbone-type (rather than layered-type, as in the T*p*CPP-based materials) arrangements of adjacent porphyrins and their efficient offset stacking along the normal direction, as observed in many other porphyrin-based solids.[13]

(13) (a) Byrn, M. P.; Curtis, C. J.; Hsiou, Y.; Khan, S. I.; Sawin, P. A.; Tendick, S. K.; Terzis, A.; Strouse, C. E. *J. Am. Chem. Soc.* **1993**, *115*, 9480−9497. (b) Krishna Kumar, R.; Balasubramanian, S.; Goldberg, I. *Inorg. Chem.* **1998**, *37*, 541−552.

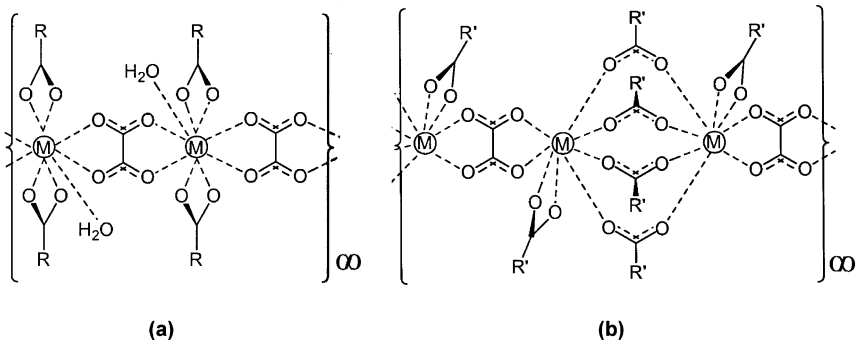

Figure 10. Schematic illustration of the continuous coordination patterns in (a) **5** and (b) **6**. In the two structures, the oxalate anions are incorporated as spacers into the binding scheme. "M" symbolizes the Dy^{III} ions, whereas "R" and "R′" indicate T*m*CPP (in **5**) and T*p*CPP (in **6**) frameworks associated with the COOH/COO^- group they are attached to. (CN = 9 in **5** and CN = 8 in **6**.) Dashed lines denote the coordination bonds.

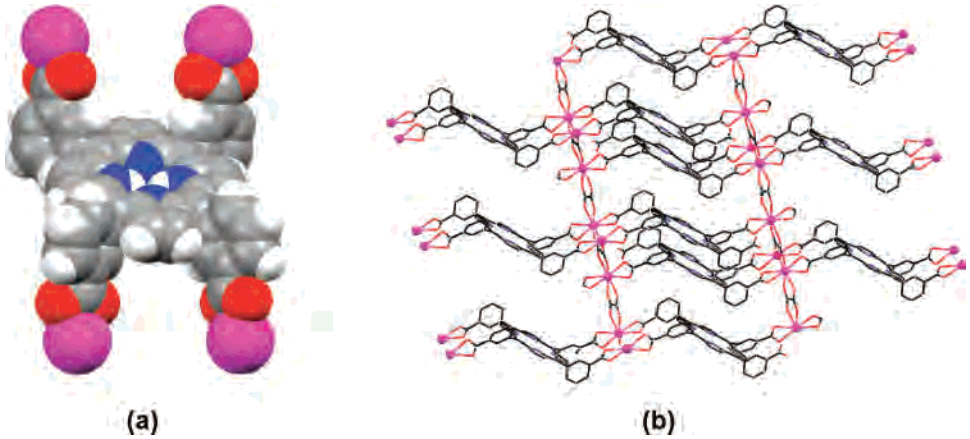

Figure 11. (a) Space-filling illustration of deprotonated chair-shaped T*m*CPP unit coordinated at its four corners to four Dy^{III} ions (largest spheres) in **5**. Note the overall chairlike conformation. (b) Partial view of the coordination polymerization in **5**, showing the oxalate ions incorporated into the binding scheme. Note the cascaded nature of the polymeric aggregate. Small spheres denote the metal ions. H atoms and water ligands are omitted for clarity.

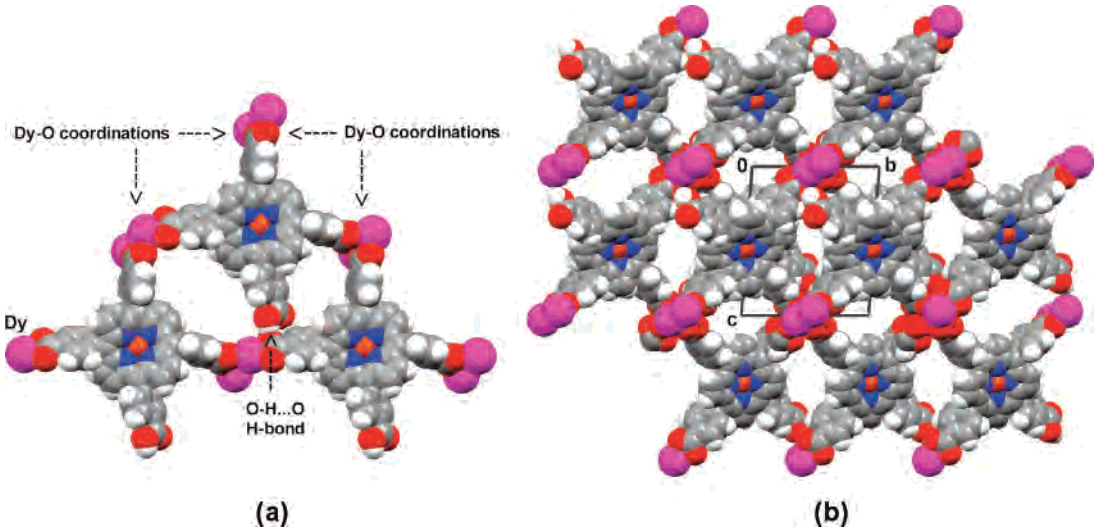

Figure 12. (a) The intermolecular interaction mode between the T*p*CPP moieties and Dy^{III} ions (largest spheres) in **6**. Note that two of the carboxylate groups of each porphyrin unit coordinate to two different metal ions, whereas the third one doubly binds to a third metal ion. The fourth carboxylic function hydrogen bonds to the latter carboxylate of a neighboring species. (b) Crystal structure of the coordination polymer lattice **5** viewed down the *a* axis (space-filling), showing the intralattice channel voids that perforate the polymeric architecture. The coordination arrays defined in Figure 10b that involve the oxalate spacers propagate as construction pillars perpendicular to the projection shown, parallel to these channels, and parallel to the *a* axis.

An interesting diversion from this line of direct lanthanide−porphyrin coordination polymerization was encountered in a small number of examples. It appears that even in the harsh hydrothermal reaction conditions, the oxalate anions of the original lanthanide reagent (provided as an oxalate salt) are not always fully replaced by the porphyrin tetraacid ligands. In such cases, the oxalate ions, which bear two carboxylate functions, become part of the polymeric coordination scheme. Typical coordination patterns of the T*m*CPP as well as T*p*CPP building blocks with Dy^{III} metal that

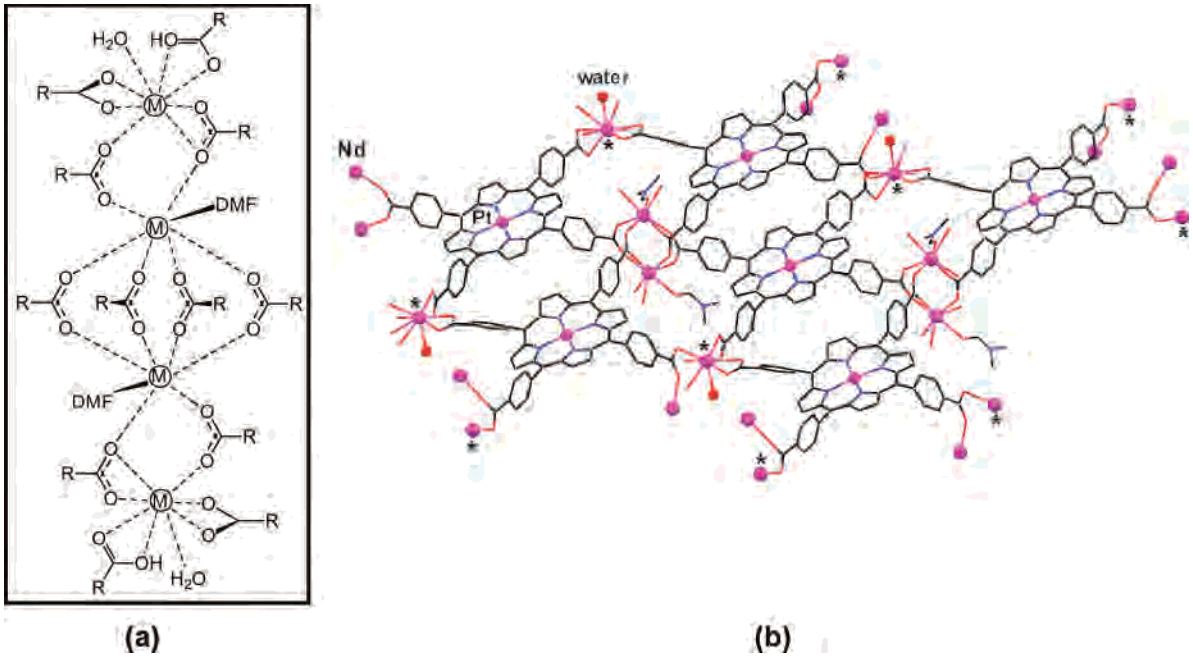

Figure 13. (a) Schematic presentation of the tetranuclear lanthanide−porphyrin coordination synthon in **7**. "M" symbolizes the Nd^{III} ions, whereas "R" represents the Pt−T*p*CPP framework associated with the COOH/COO^- group it is attached to. Dashed lines denote the coordination bonds with Nd−O distances ≤2.65 Å. (b) Layered fragment of the metalloporphyrin network tessellated by metal−ligand coordination. The Nd and Pt ions, as well as the water ligands, are denoted by small spheres. Asterisked atoms mark the outer ions in the tetranuclear cluster. The sticks protruding from the Nd metal ions represent O sites of carboxylic/carboxylate functions of adjacent porphyrin species within this layer or in neighboring layers above and below.

incorporate oxalate anions are shown in Figure 10. In these polymeric arrays, the oxalates act as spacers, binding simultaneously to two or more metal centers along the polymer.

In the 2:1 Dy−T*m*CPP compound **5**, the metal ion is coordinated to two carboxylate groups of two different porphyrin units as well as to two oxalate ions. A molecule of water complements the CN = 9 coordination sphere around Dy^{III} (Table 3). The porphyrin tetraacid is fully deprotonated, and each of the carboxylate functions doubly coordinates to a different metal ion (Figure 11), thus affording a 3D architecture. Two of these functions are directed above the core macrocycle and two below it, imparting a cascaded character to the polymeric arrays. Crystal packing of the latter is associated with the presence of considerably larger intralattice voids than in the previous examples (Tables 1 and 2).

The formulation of closely related coordination polymers, utilizing the free-base T*p*CPP platform, has been described earlier.[9] The reported examples referred to materials involving the free-base entity. Complementary information provided below relates to materials incorporating metalloporphyrin derivatives. As indicated in Figure 10b, Cu−T*p*CPP was also found to polymerize with dysprosium oxalate in a 1:1 ratio and to yield extended arrays of 3D topology (**6**). The oxalate anions are part of the polymeric arrays in this structure as well. Yet, the observed connectivity pattern in **6** is markedly different than in **5**, possibly due to the different directionality of the para-substituted COOH/COO^-, which now diverge in lateral directions with respect to the mean plane of the porphyrin moiety. Adjacent metal ions along the polymeric chains are alternately bridged by either oxalate anions or four carboxylate functions. They complement the coordination sphere to CN = 8 by doubly coordinating a carboxylate group of an additional porphyrin unit. Space-filling illustrations of the binding mode and the overall crystal architecture are given in Figure 12.

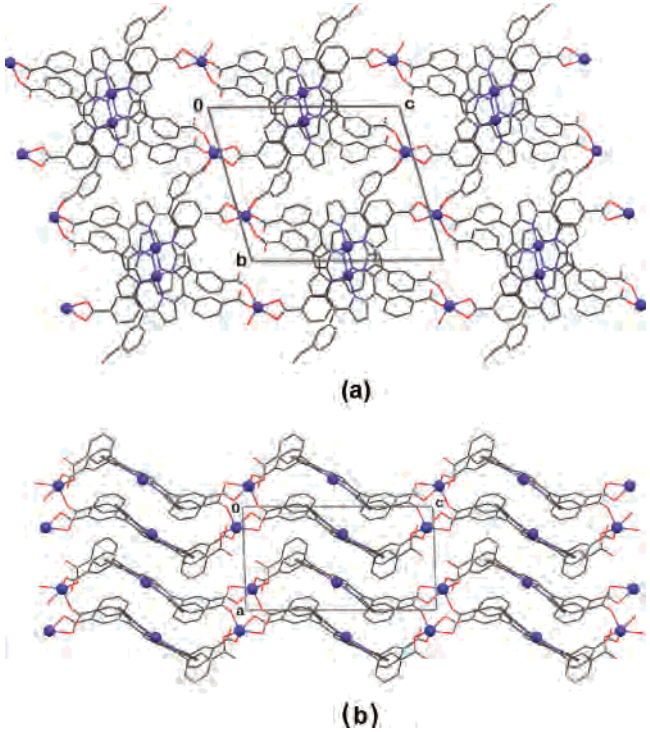

Figure 14. Crystal structure of **8**. (a) Projection down the *a* axis, showing Co-bridged 2D bilayered porphyrin assemblies. Note that the cobalt linkers are five-coordinate. (b) Projection down the *b* axis, illustrating van der Waals stacking of these bilayers along *a* without any coordination interactions between them. Small spheres represent the cobalt ions. The solvent dimethylamine and water species trapped in the interporphyrin voids are omitted.

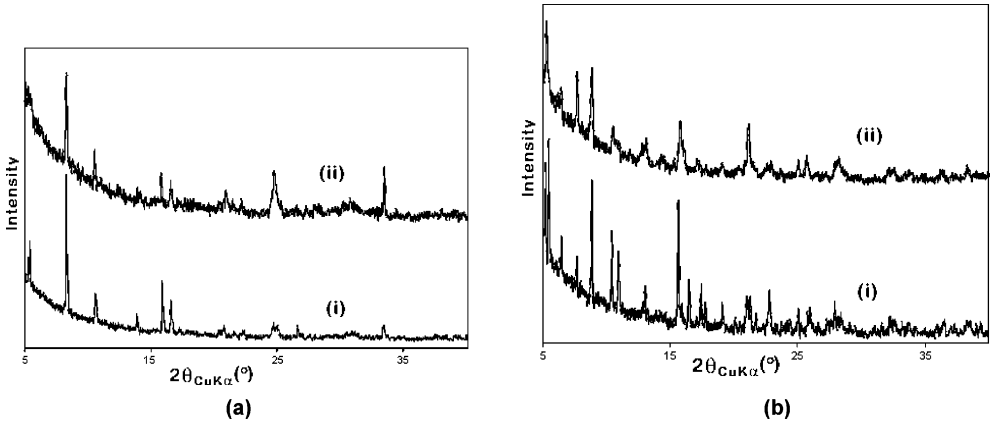

Figure 15. Powder XRD patterns of (a) **1** and (b) **4**: (i) Original reaction product (identical pattern is obtained after this material is exposed to open air for several hours). (ii) After subsequent annealing of the powders analyzed in i at 200 °C for 3 h. All spectra were measured at room temperature.

In a related reaction of $Nd_2(oxalate)_3$ with Pt−T*p*CPP, a complete displacement of the oxalate anions from the coordination sphere of the metal by the porphyrin carboxylate groups has been accomplished. The resulting architecture is nearly isomorphous with that observed for the coordination polymer of free-base T*p*CPP with Nd^{III} and other lanthanide ions[9] and therefore will be referred to only briefly here. The lanthanide−T*p*CPP direct coordination is confined to clusters of 4 metal ions and COOH/COO^- sites of 12 different porphyrin moieties (Figure 13a). Within the tetranuclear assembly, each of the "inner" metal ions coordinates to six carboxylate functions and an additional DMF ligand (CN = 7). These ions are bridged by four carboxylates from different sides, and the distance between them is 4.17 Å. The "outer" ions on either side of the cluster have a more complex coordination environment (CN = 8), linking to four carboxylate/carboxylic acid functions and a water molecule. Only two carboxylate groups bridge between the outer ion and an adjacent inner ion (at a distance of ∼4.09 Å). The supramolecular architecture is composed of layered multiporphyrin domains (Figure 13b), which are tessellated together into single-framework architecture by the bridging tetranuclear assemblies. Within such layers, the porphyrins are interlinked into an open network through a pair of the two inner-metal ions, an outer ion of a tetrameric cluster pointing upward, or an outer ion of a tetrameric cluster pointing downward. Neighboring carboxylate-bridged tetranuclear clusters span in an alternating manner over different three-layer sets of Pt−T*p*CPP. They are shifted vertically with respect to one another, imparting "pillared" single-framework connectivity features to the thus-formed polymeric architecture. The overall structure of the stacked porphyrin layers is characterized by the presence of parallel channel voids, which propagate through the crystal in a normal direction. As in the previous example, one of the two metalloporphyrin units of the asymmetric unit adopts a considerably saddled conformation (the other species resides on a crystallographic two-fold axis and is nearly planar), although in general the four-coordinate Pt−T*p*CPP macrocycle tends to be planar.[6b] The dihedral angles between the pyrrole rings located across the macrocycle in **7** are 16.3(5)° and 18.0(5)°.

All the above solids are stable at ambient conditions without significant deterioration for days and weeks, as confirmed by repeated diffraction experiments. Spectroscopic analysis of their solutions in DMSO (DMSO = dimethylsulfoxide) (these solids once formed are sparingly soluble in other less-polar solvents) did not show any unique absorption or fluorescence features other than those that are characteristic of the individual components. Correspondingly, there is no evidence that the lanthanide−TCPP coordination aggregates (either polymers or oligomers) are present in solution, and their excited-state properties could not be characterized.

As T*m*CPP formally represents a new building block for supramolecular assembly, its coordination polymers with more-common third-row transition metal ions have not been reported before. We illustrate here one such example (**8**), which provides further support of the idea that lanthanide ions are better suited than the lighter transition metals for formulations of 3D single-framework architecture.[9] Figure 14, shows the connectivity scheme obtained after reacting T*m*CPP with cobalt acetate. In this reaction, the Co^{III} ions are inserted within as well as between the porphyrin units, the latter coordinating to the peripheral carboxylate functions and forming polymeric arrays. However, due to the smaller size and lower coordination affinity of Co^{III} linkers (in comparison with the trivalent lanthanide ions), the obtained coordination polymers are characterized by *two-dimensional* connectivity only, with the cobalt ion connecting to four different carboxylate groups (and five O atoms). The chairlike geometry of the porphyrin ligand that allows optimal networking with neighboring species is preserved in **8**.

The thermal stability of the T*m*CPP materials has been assessed by thermal gravimetric (TGA) and X-ray powder diffraction (XRD) techniques. The TGA (accompanied by differential thermal analysis, DTA) patterns of compounds **1**, **2**, **4** (**3** is isomorphous to **4**), and **5** show that after the evaporation of the solvent adsorbed on (or near) the crystal surface below ∼75−85 °C, the lattice-included water and DMF species (about 10% of the dry crystal mass in **1**, **2**, and **4** but only about 4% in **5**) are lost within the 90−200 °C temperature range (see the Supporting Information).

All compounds then maintain their mass with only a minor degradation (which is somewhat more prominent in **2** than in the other solids), until slightly above 350 °C, before disintegrating into a black powder upon further heating. Supplementary data is provided by XRD powder patterns of solids **1** and **4**. They show that the characteristic "fingerprint" for these two compounds remains unchanged upon exposure for hours to open air. Moreover, similar spectra are obtained after subsequent annealing of the analyzed powders at 200 °C for 3 h (Figure 15). The above observations attest to the marked stability of the lanthanide-tessellated T*m*CPP frameworks.

Conclusion

The synthesis of framework hybrid coordination polymers composed of the *meso*-tetra(carboxyphenyl)porphyrin species and various lanthanide metal ions has been demonstrated. The main ideas behind the successful construction of these materials involve the unique topology of the T*m*CPP and T*p*CPP building blocks of tetradentate functionality and square-planar geometry, the affinity for high CNs of the lanthanide ions, their tendency to form polynuclear acetate/oxalate-bridged clusters,[10] and specific experimental conditions that induce the formation of polynuclear coordination synthons and thus impart stability to the polymeric assemblies that form.[11,12] The continuous coordination scheme is effective with both the meta and para isomers of the porphyrin tetraacid as well as with their free-base and metalated derivatives. Structures based on the T*m*CPP and T*p*CPP scaffolds differ in the topology of the supramolecular organization, generally consisting of offset-stacked wavy-corrugated vs flat-layered arrays of the porphyrin species due to the different direction of the lanthanide−carboxylate bonds. Correspondingly, the solvent-accessible channel voids that perforate the corresponding structures are wider in the T*p*CPP (0.5−0.6 nm) than in the T*m*CPP (0.4−0.5 nm) materials. Compounds **1**−**7** consist of *truly* 3D and open-coordination polymer frameworks rarely obtained before in porphyrin-based solids by systematic design.[7,8] On the other hand, only 2D polymeric frameworks are represented in compound **8**, in which Co ions were used as T*m*CPP-interporphyrin linkers. The lanthanide−T*m*CPP frameworks reveal high thermal stability, similar to that of their T*p*CPP analogues.[9] These results provide an expansion of our pioneering application of the uniquely versatile tetra(carboxyphenyl)porphyrin platform in formulations of zeolite-like architectures with the aid of other bridging auxiliaries (metal ions, as well as organic ligands).[5,6] There are still some drawbacks to the above-reported results at this stage. We are unable to control the nuclearity of the lanthanide−carboxylate synthons that form. Then, the presently formulated structures show somewhat limited porosity, which may be unsuitable for storage and transport applications. It is anticipated, however, that similar crystal-engineering concepts utilizing the lanthanide-bridging reagents along with their high binding affinity to carboxylate organics can be applied in attempts to develop more open and more uniformly structured metal−organic framework solids.

Experimental Section

Molecular and Supramolecular Synthesis. All starting reagents (Aldrich), Cu and Pt 5,10,15,20-tetrakis(4-carboxyphenyl)porphyrin (Cu−T*p*CPP and Pt−T*p*CPP, Porphyrin Systems), various lanthanide salts (often contaminated by the presence of other ions, Aldrich), and reagent-grade solvents (Aldrich, Merck) were procured commercially and used without further purification. The 5,10,15,20-tetrakis(3-carboxyphenyl)porphyrin (T*m*CPP) was synthesized locally by the modified Lindsey method,[14] involving KOH hydrolysis of the corresponding carbomethoxyphenyl intermediate.

Thus, 2 g (0.123 mol) of 3-carbomethoxybenzaldehyde and 0.85 mL of distilled pyrrole (0.123 mol) were added to 800 mL of freshly distilled CH_2Cl_2 and purged with argon for 20 min. Then, BF_3 etherate (0.4 mL, 3.16 mmol) was added via syringe, and the reaction mixture was protected from light. After stirring at room temperature for 1 h, 2.3 g (9.35 mmol) of *p*-chloranil was added slowly in the solid form and the solution was stirred for a further 90 min. The solution was concentrated to a small volume using a rotary evaporator. To this solution, dry silica gel (30 g, 60−200 mesh) was added and the slurry was evaporated to give a dry black powder, which was loaded on a silica column using $CHCl_3$ and eluted with 5−8% acetone in $CHCl_3$ to remove any poly(pyrrole) impurity. It was then further purified on a silica column using 4% acetone in $CHCl_3$ and recrystallized from a 1:4 $CHCl_3$/methanol mixture (v/v). Yield: 0.62 g (24%). ^{1}H NMR ($CDCl_3$): 8.89 (s, 4H), 8.79 (s, 8H), 8.49 (d, $J = 7.84$ Hz, 4H), 8.40 (d, $J = 7.68$ Hz, 4H), 7.85 (t, $J = 7.7$ Hz, 4H), 3.98 (s, 12H), −2.80 (s, 2H). UV−vis in THF: λ_{max}(log ϵ) nm 417(5.73), 513(4.44), 547(4.05), 590(3.94), 646(3.62). FAB-mass spectrum (*m*/*z*) for $C_{52}H_{38}N_4O_8$: found, 847; calcd, 846.90.

In the next stage, 0.25 g (0.295 mmol) of the latter product was dissolved in 50 mL of THF. To this, 1.65 g (0.0295 mol) of KOH in 1 mL of water was added and heated at 75 °C for 14 h. At the end of this period, THF was removed by rotary evaporation. The crude porphyrin was treated with 50 mL of 2 N HCl solution yielding a green precipitate, which was filtered, washed with water, and dried. Protonated porphyrin was neutralized by adding 6 mL of pyridine and subsequently removed by vacuum distillation. Then purple solid was washed with water and dried under vacuum. Yield: 0.23 g (98%). ^{1}H NMR ($CDCl_3$): 13.2 (s, 4H), 8.78 (s, 8H), 8.66 (s, 4H), 8.51 (dd, $J = 4.1$ Hz, $J = 1.8$ Hz, 4H), 8.44 (dd, $J = 6.2$ Hz, 4 H), 8.37 (d, $J = 8$ Hz, 4H), 7.92 (t, $J = 7.7$ Hz, 4H), −2.98 (s, 2H). UV−vis in THF: λ_{max}(log ϵ) nm 417(5.64), 513(4.32), 547(3.93), 590(3.79), 647(3.71). FAB-mass spectrum (*m*/*z*) for $C_{48}H_{30}N_4O_8$: found, 791; calcd, 790.79.

A general procedure for the preparation of the lanthanide−porphyrin polymers **1**−**4**, **6**, and **7**: 4−5 mg (∼0.005 mmol) of T*m*CPP, Cu−T*p*CPP, or Pt−T*p*TCPP was dissolved in 1.0−1.5 mL of DMF (*N*,*N*′-dimethylformamide). To this, 1.2−1.5 equiv (1.5−3.0 mg) of lanthanide(III) acetate/oxalate/chloride hydrate dissolved in ∼1 mL of 0.8 N hydrochloric acid was added The resulting reaction mixture was sealed in a small reactor, heated to 150 °C by gradually raising the temperature at a gradient of 0.5 °C/min, and maintained at 150 °C for 50 h. Very slow cooling of the reactor to ambient conditions, yielding X-ray quality crystals, followed this. They were found to contain, in addition to the lanthanide−porphyrin coordination polymers, a considerable amount of the crystallization solvent in the lattice. For the preparation of compounds **5** and **8**, 4.6 mg (0.006 mmol) of T*m*CPP was dissolved in 1 mL of DMF, and then 0.5 mL of 0.2 N aqueous KOH was

(14) Lindsey, J. S.; Schreiman, I. C.; Hsu, H. C.; Kearney, P. C.; Margueretazz, A. M. *J. Org. Chem.* **1987**, *52*, 827−836.

added to enhance the deprotonation of the porphyrin tetraacid. To this, 4.1 mg of $Dy_2(oxalate)_3$ (for **5**) or 4.3 mg of $Co(acetate)_3 \cdot 4H_2O$ (for **8**) in 0.4 mL of distilled water was added, followed by the addition of 0.05 mL of pyridine to increase solubility. These reaction mixtures were placed in sealed reactors, gradually heated to 150 °C, and maintained at this temperature for 50 h. Very slow cooling (0.5 °C/5 min) of the reactors to room temperature yielded X-ray quality crystals. The uniform identity of the formed crystal lattices (**1**−**8**) in a given reaction was confirmed in each case by repeated measurements of the unit-cell dimensions from different single crystallites.

Crystallography. The X-ray measurements (Nonius KappaCCD diffractometer, Mo Kα radiation) were carried out at ca. 110 K on crystals coated with a thin layer of amorphous oil to minimize crystal deterioration, possible structural disorder, and related thermal motion effects and to optimize the precision of the structural results. These structures were solved by Patterson (*DIRDIF-96*) and direct methods (*SHELXS-86*, *SIR-92/97*) and refined by full-matrix least squares (*SHELXL-97*).[15] All non-hydrogen atoms were refined anisotropically. The hydrogen atoms were located in idealized/calculated positions and were refined using a riding model, with $U_{iso} = 1.2$ or $1.5\ U_{eq}$ of the parent atom. Structures **1**−**7** were found to represent an open 3D lanthanide−porphyrin lattice with channel voids accommodating the noninteracting crystallization solvent. The latter was found highly diffused in these voids, showing randomly scattered residual electron-density peaks (2−8 e/Å^3) and could not be reliably modeled by discrete atoms. Correspondingly, the contribution of the disordered solvent moieties was subtracted from the diffraction pattern by the squeeze procedure (commonly used in similar situations),[16] allowing smooth convergence of the crystallographic refinements to acceptable low *R* values and precise description of the metal−porphyrin frameworks. Structure **8** consists of 2D (rather than 3D) polymeric arrays sustained by the bridging-Co ions. Molecules of dimethylamine and water were found to be included in the crystal lattice.

Acknowledgment. This research was supported by The Israel Science Foundation (Grant No. 254/04). The authors thank Dr. Y. Rozenberg and Dr. D. Golodnitsky for the XRD and TGA measurements.

Supporting Information Available: X-ray crystallographic files in CIF format for the eight crystalline solids **1**−**8**. TGA and DTA diagrams for **1**, **2**, **4**, and **5**. This information is available free of charge via the Internet at http://pubs.acs.org

IC0701099

(15) (a) Beurskens, P. T.; Admiraal, G.; Beurskens, G.; Bosman, W. P.; Garcia-Granda, S.; Gould, R. O.; Smits, J. M. M.; Smykalla, C.; The *DIRDIF-96* Program System; Crystallography Laboratory, University of Nijmegen: Nijmegen, The Netherlands, 1996. (b) Altomare, A.; Burla, M. C.; Camalli, M.; Cascarano, M.; Giacovazzo, C.; Guagliardi, A.; Polidori, G; *SIR-92/97*, *J. Appl. Crystallogr.* **1994**, *27*, 435−436. (c) Sheldrick, G. M.; *SHELXS*-86 and *SHELXL-97*. Programs for the Solution and Refinement of Crystal Structures from Diffraction Data; University of Göttingen: Göttingen, Germany, 1997.

(16) Spek, A. L. *J. Appl. Crystallogr.* **2003**, *36*, 7−13.